Computers & Industrial Engineering 204 (2025) 111110

Contents lists available at ScienceDirect

Computers & Industrial Engineering

journal homepage: www.elsevier.com/locate/caie

Human control mode enables accurate real-time risk warning in human–machine systems

Chongfeng Li [a], Xing Pan [a,*], Linchao Yang [b], Jun Wang [c], Haobing Ma [a]

[a] School of Reliability and Systems Engineering, Beihang University, 37 Xueyuan Road, Haidian, Beijing 100191, China
[b] School of Economics and Management, North China Electric Power University, Beinong Road, Changping, Beijing 102206, China
[c] School of Economics and Management, Beihang University, 37 Xueyuan Road, Haidian, Beijing 100191, China

ARTICLE INFO

Keywords:
Industry risk
Human–machine systems
Human-centric risk warnings
Human control
Machine learning

ABSTRACT

Data-driven risk analysis serves as an essential approach to risk mitigation in human–machine systems. Presently, risk management rooted in data often depends on labels extracted from risk outcomes, accentuating a causative risk management paradigm. However, these labels frequently fall short in capturing the dynamic evolution of risks in real-time, especially accounting for the impact of human intervention on risk dissemination. In striving for greater precision in real-time risk prediction within human–machine systems, human control is identified as a pivotal factor in shaping risk progression. A precise warning model is devised based on human control patterns, discerned through clustering control data focusing on "timeliness," "stability," and "coordination." This methodology facilitates the development of machine learning-driven warning models. The viability of the proposed approach is substantiated through a case study involving aircraft landing mishaps. This research furnishes a conceptual framework and procedural guidelines to propel risk analysis within human–machine systems, with an emphasis on human-centric risk warnings across diverse industrial contexts.

1. Introduction

With the increasing complexity of human–machine systems, the key risk factors of human–machine systems are gradually shifting from the machine itself to the human–machine interaction process (Hollnagel, 2018). Currently, data-driven risk warning is gradually being applied to various human–machine system domains, such as manufacturing, transportation, and aviation industries (Aziz & Dowling, 2019; Choi et al., 2016). Real-time warning is a viable method to decrease accident risk by providing timely alerts to drivers about potential risk (Li, Zhao, et al., 2020; Oh et al., 2005). The core of data-driven risk warning lies in learning the risk patterns from historical accident data and issuing advance warnings before accidents occur (Guo et al., 2022). The accuracy of data risk labels directly impacts the effectiveness of the warnings. As illustrated in Fig. 1, human–machine system risk labels mostly originate from risk outcomes, i.e., using past accidents to calibrate risk labels, without considering the influence of human control. However, the impact of human control on risks is increasingly uncertain, particularly concerning real-time warnings. If real-time changes in human control are not considered, accurate predictions of risk evolution cannot be obtained. Therefore, current risk warnings based on risk outcomes as data labels overlook the uncertain risk control centered around human control. From a data-driven perspective, this approach introduces incorrect risk classification samples, like FN and FP in Fig. 1, leading to a decrease in the accuracy of the warning models. Thus, combining risk resistance based on real-time warning and human control is essential to fully utilize risk data to enhance the prevention and control capabilities of accidents.

The issues reflected in Fig. 1 exist in various domains where human control is central, such as automotive driving systems (Matsuo et al., 2022b; Sun et al., 2016), aviation transportation systems (Guo et al., 2022; Li et al., 2023), industrial manufacturing systems (Bertoncel et al., 2018), and nuclear industries (Hamer et al., 2021; Horita et al., 2018), where risks are prevalent. Taking aviation risks as an illustration, the global civil aviation industry has witnessed a resurgence following the COVID-19 pandemic. However, amidst the annual increase in flight frequencies and transportation capacities, there has been a surge in aviation accidents, resulting in irreparable human casualties and economic losses (ICAO, 2024). With the continuous development of computer technology and air-to-ground data communication technology, some countries have already achieved data-driven aviation risk management (Li et al., 2023), However, there also exists a problem of not considering the impact of human control on the effectiveness of real-

* Corresponding authors.
E-mail address: panxing@buaa.edu.cn (X. Pan).

https://doi.org/10.1016/j.cie.2025.111110
Received 22 April 2024; Received in revised form 25 February 2025; Accepted 2 April 2025
Available online 11 April 2025

Nomenclature

A	Accuracy of Machine Learning (\)
AP	Aircraft performance parameters (\)
ACS	Auxiliary control sequence (\)
AD	Machine state deviations (\)
ALT	The altitude of an aircraft relative to the ground (m)
B	Pilot behavior parameters (\)
C_D	Drag coefficient (\)
C_L	Lift coefficient (\)
DD	Task degree of difficulty (\)
D_{HCM}	Data for HCM prediction (\)
DP	Decision performance (\)
E	Environment parameters (\)
EC	Environment Condition (\)
$Flap$	Flaps configuration (\)
F_1	F_1 score of Machine Learning (\)
g	Gravity acceleration (m/s^2)
H	Human control parameters (\)
HC	Human control data (\)
HCM	Human control mode (\)
HCS	Human control sequences (\)
HC_T	Timeliness of ***HCS*** (\)
HC_S	Stability of ***HCS*** (\)
HC_C	Coordination of ***HCS*** (\)
k	k-SC clustering number (\)
m	Gross weight of aircraft (kg)
M	Machine parameters (\)
MA	Machine factors (\)
MCS	main control sequence (\)
P	Precision of Machine Learning (\)
P_S	Static pressure (Pa)
QAR	Quick Access Recorder (\)
R	Recall rate of Machine Learning (\)
S	Takeoff distance (m)
SA	Situation awareness (\)
S_W	Wing reference area (m^2)
SOP	Standard Operating Procedure (\)
t	Time of operations (s)
TH	Task hardness (\)
T_S	Static temperature (°C)
TP	Track deviation (\)
V_A	The speed of aircraft indicated by instrument (m/s)
V_{REF}	The reference speed of aircraft in Landing (m/s)
V_W	Tailwind speed (m/s)
WV	Warning variables (\)
WP	Warning points based on WV (\)
ρ	Atmospheric density (Kg/m^3)

time warnings. This endeavor aims to augment the performance of real-time warning models for aviation risk, thereby enhancing proactive safety measures.

Therefore, this study targets the influence of human control on risk evolution in human–machine systems. A real-time warning approach is proposed for risks based on human control modes (HCM) and apply it to the research on aviation industry. The primary contributions of this research are as follows:

1) Introduction of a real-time warning framework for risk in human–machine systems based on HCM.
2) Exploration of typical HCM through the analysis of "timeliness," "stability," and "coordination" of human control data.
3) Development of a risk warning method, encompassing methods for HCM real-time analysis and risk prediction model by machine learning.
4) Validation of the effectiveness and practical significance of the proposed approach through its application to common aviation risks in aviation industry.

The research is divided into the following specific sections. Section 2 is a literature review, which starts from the limitations of risk warning research in human–machine systems and proposes the perspective of real-time warning considering human control. Section 3 introduces a real-time risk warning method for human–machine systems based on HCM, including the mining of HCM, the prediction of HCM, and the real-time risk warning based on HCM. Section 4 uses the example of civil aviation landing risk to illustrate the effectiveness of the proposed method. The limitations of the current research and the conclusions are explained in Section 5 and Section 6, respectively.

2. Literature review

2.1. Accident prediction and risk warning

Risk warning is a valuable way in enhancing system safety by providing timely alerts and predictive warnings to human operators (Ding et al., 2013). Risk warning, based on risk prediction, inform people of the forecasted risks ahead of time, allowing for timely risk control to prevent severe accident consequences (Saleh et al., 2013). The

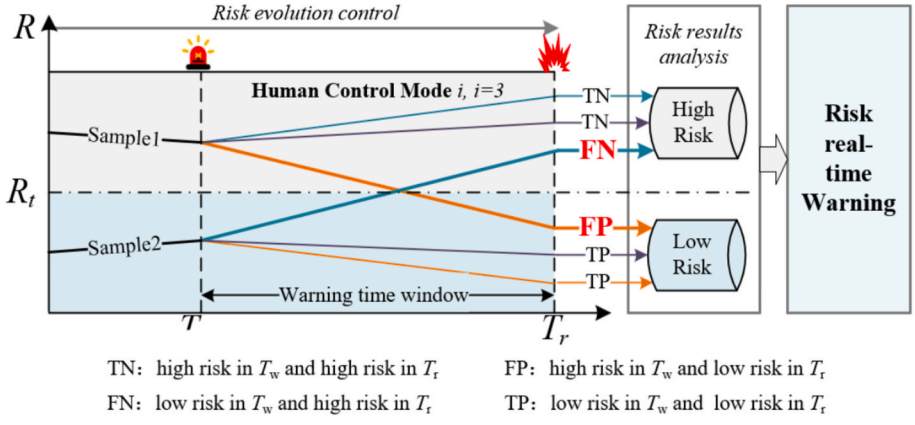

Fig. 1. The background of research gap.

essence of risk warning lies in providing relatively accurate risk information at appropriate warning times, and a key aspect to achieving this goal is understanding the evolution mechanism of risks as thoroughly as possible. However, with the ongoing complexity of socio-technical system structures, the uncertainty surrounding accident evolution mechanisms continues to increase. Currently, data-driven approaches and human expertise offer effective means to address the uncertainty in accident evolution. Various methods have emerged, including rule-based warnings (Wu & Chen, 2008), probability model-based warnings (Kelly & Krzysztofowicz, 1994), machine learning-based warnings (Ghoul et al., 2023; Zhang et al., 2022), deep learning-based warnings (Bury et al., 2021), and Machine learning and deep learning are important technologies of AI driven risk management. Based on the accessibility of warning data and the maturity of data transmission technology, data-driven warnings can be classified as proactive warnings and real-time warnings, with real-time warnings being more effective for risk prevention.

For typical human–machine systems, most related real-time warning research focuses on using historical accident outcomes as risk labels and pays attention to risk warnings based on system performance data (Li, Gan, et al., 2020; Li et al., 2018; Matsuo et al., 2022a; Yu et al., 2021). However, the current research rarely considers the influence of human control on the risk evolution in historical accident data. As a result, it has been challenging to derive relatively accurate risk warning models based on historical data. Nowadays, extensive accident statistics from various industries demonstrate the influence of real-time human control on risk evolution (IATA, 2023; Poynter, 2023; Youlong et al., 2023). Therefore, it is necessary to consider the influence of human control on real-time warning results, which is possible to improve the accuracy of risk warning and avoid more losses.

2.2. Risk evolution and human control

As mentioned earlier, the increasing complexity of socio-technical systems has introduced a high level of uncertainty to the mechanisms underlying risk evolution, which is influenced by factors such as "human-machine-environment-management." Against this backdrop, real-time risk warnings not only need to consider changes in system performance parameters but also pay attention to the human control factors that trigger those changes (Summala, 1996). Taking the aviation safety domain as an example, human control plays a critical role in flight safety systems (Dolores and Gracja, 2018; Reason, 1990). Some researchers have suggested that human pilot errors contribute to over 60 % of aviation accidents (Jarvis & Harris, 2010; Shappell et al., 2017). Statistics from the International Air Transport Association (IATA) for 2016–2020 indicate that crew-related factors contributed to approximately 46 % of aircraft accidents (IATA, 2021). Relevant data from sectors such as road transportation (Dzinyela et al., 2024; Poynter, 2023) and nuclear power plants (Youlong et al., 2023) also consistently demonstrate the significant impact of human control on risk.

In typical human–machine systems, human control over the system is the output of their cognitive processes, and the results directly influence the risk evolution of the entire system. Human Reliability Analysis (HRA) is a field specifically dedicated to studying the impact of human behavior on system risk, including first-generation HRA, second-generation HRA (Swain, 1990), and third-generation HRA methods (Pan et al., 2017). Second-generation HRA models, represented by methods such as the ATHEANA (Commission, 1999), CREAM (Hollnagel, 1998), and ADS-IDAC (Mosleh & Chang, 2004), explain human control behavior by establishing cognitive models.

Among them, Wickens introduced the concept from the field of information processing, treating humans as information processors, and proposed the HIP Model (Wickens et al., 2021). The HIP describes the human cognitive process from the perspective of information flow, considering it as the flow of cognitive information in the human brain, comprising three main stages: "input-processing-output." The information processing model explains the mechanism of human control behavior from the perspective of information flow and can be seen as a key mechanism influencing risk evolution in the human–machine systems. Existing research based on cognitive models often assess human error probability by evaluating PSFs (French et al., 2011). Few studies have combined cognition-based human control processes with the real-time operation of machines, especially risk evolution. However, it is precisely the differences in real-time cognitive processes that lead to variations in human control outcomes, directly affecting the results of risk warnings. Therefore, as shown in Fig. 2, starting from the perspective of data-driven real-time warnings, it is necessary to extract variables representing human cognitive states (defined in this study as HCM) from human control data. Furthermore, real-time analysis of HCM should be conducted in the process of real-time warnings to fully identify the impact of human control on risk evolution.

In this study, human control, in conjunction with real-time risk warning, is regarded as a crucial mechanism for safety of human–machine systems. This approach is expected to address the existing issue of inaccurate warnings resulting from the failure to consider human control in real-time risk alerts. It holds significant implications for reducing risks in various human control systems by comprehensively considering human factors and enhancing the accuracy and effectiveness of warnings.

3. Method

This section firstly presents a framework for real-time risk warning based on HCM, which illustrates the data sources and the overall idea of achieving real-time risk warning through human control. Secondly, it provides an HCM mining method for human control from three dimensions: "timeliness," "stability," and "coordination" of human control data. Finally, a system risk warning method using machine learning is proposed based on HCM.

3.1. HCM-based framework for real-time risk warning

The real-time risk warning framework for risks based on HCM is illustrated in Fig. 3. Initially, the disciplinary equation $f(\boldsymbol{H}, \boldsymbol{M}, \boldsymbol{E})$ of typical human–machine systems is referenced, and corresponding parameters from the three dimensions of the "human–machine-environment" are selected as inputs for the entire model. Essentially, the performance of the system can be calculated in real-time through the disciplinary equation of the physical system. However, due to the influence of human control, the required constraints and parameter specifications of the disciplinary equation for the physical system are often not accurately met. Therefore, the entire real-time warning framework takes a data-centric approach, based on data exploration of the general patterns of risks, especially quantifying the influence of human control on risks. Ultimately, the framework achieves real-time risk warning of accidents based on HCM.

Based on the input parameters, data-based HCM mining, HCM analysis, and real-time risk warning are performed separately. The offline HCM mining is conducted based on main control sequence (***MCS***) and auxiliary control sequence (***ACS***), including the calculation of data features and clustering. The purpose is to identify the typical modes of human control in the current system and form HCM labels. The real-time HCM analysis model considers factors such as human cognition (situation awareness, control performance, and task difficulty), machine state factors, and environmental factors. Based on machine learning models, a real-time HCM analysis method is constructed to analyze the selected HCM used by humans in real-time operation. Furthermore, a corresponding risk warning machine learning model is built based on the selected HCM to achieve risk warning considering human control.

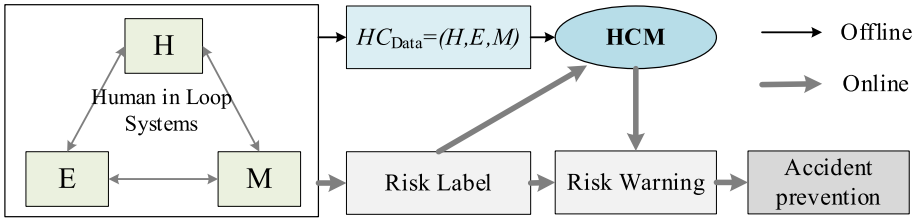

Fig. 2. Risk warning concept based on HCM.

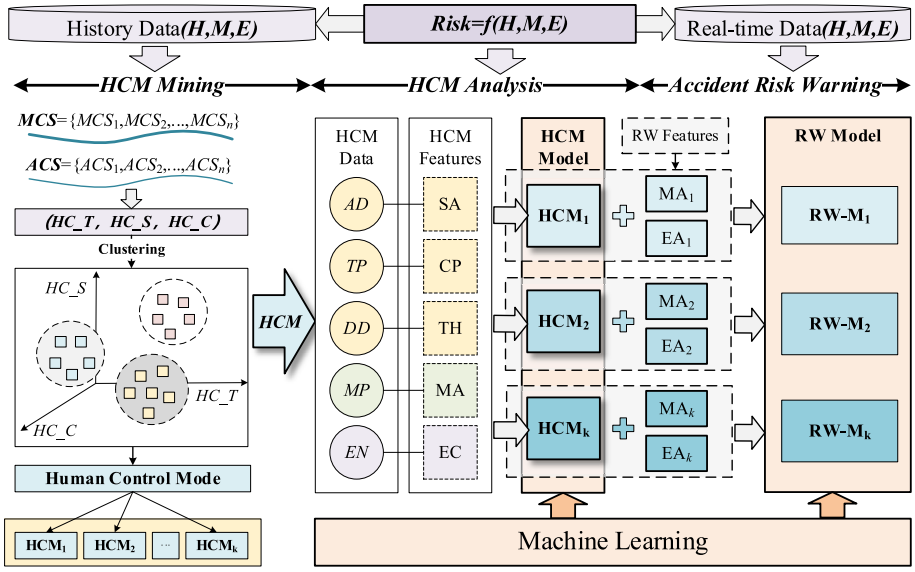

Fig. 3. The framework of risk warning concept based on HCM.

3.2. HCM mining

In this study, HCM is defined as the data characteristics exhibited by the control outcomes of typical human machine systems under specific task profiles. HCM represents the culmination of human perception of external information and the subsequent decision-making in control, influenced by the integrated factors of human psychology, physiology, and the external environment, thus inherently possessing uncertainty (Wickens et al., 2021). To further explore the influence of HCM on the risk evolution, it is imperative to quantify it. The historical data of human–machine systems encompass a wealth of human control data, reflecting human control behavior to some extent. Hence, typical HCM can be discerned through data mining techniques.

For typical human–machine systems such as automotive driving, machine operations, and aviation maneuvers, existing studies have indicated that the stability of human control can impact the risks associated with machines (Sun & Xiao, 2012). In this study, starting from the characteristics of human control data, it is considered that apart from the stability of control inputs, human control performance is also manifested in the timeliness of control, i.e., whether the designated operations are carried out at the prescribed locations in a timely manner. Moreover, human control often results from the integration of two or more types of operations, which can be simplified into ***MCS*** and ***ACS***. The coordination of them also significantly influences the outcomes of human control. Therefore, as illustrated in Fig. 4, a HCM clustering method based on timeliness, stability, and coordination is proposed. Cluster analysis is conducted in a three-dimensional space to uncover distinct HCM that can be clearly distinguished.

The specific process of mining HCM based on timeliness (*HC_T*), stability (*HC_S*) and coordination (*HC_C*) is:

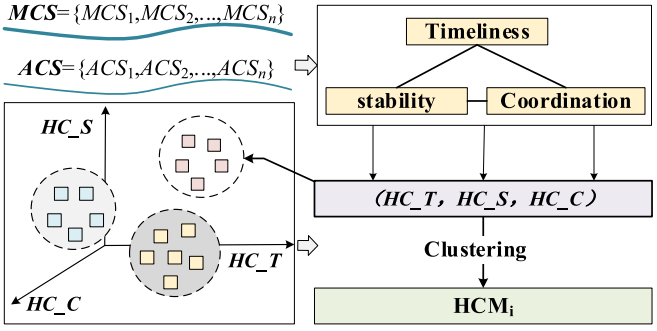

Fig. 4. HCM analysis and mining.

1) Define HCM. To obtain historical human control sequences for specific control task profiles $\boldsymbol{HCS} = [\boldsymbol{HC}_1, \boldsymbol{HC}_2, ..., \boldsymbol{HC}_i], i = 1, 2, ..., m$, where m represents the number of human control operations. In practical applications, m is generally set to 2, indicating that humans typically engage in two simultaneous operations. This study defines these as ***MCS*** and ***ACS***, thus $\boldsymbol{HCS} = [\boldsymbol{MCS}, \boldsymbol{ACS}]$, where $\boldsymbol{MCS} = [MCS_1, MCS_2, ..., MCS_n]$ represent primary operations that require a significant investment of time and resources, such as steering wheel control in cars and aircraft control yoke manipulation; $\boldsymbol{ACS} = [ACS_1, ACS_2, ..., ACS_n]$ represent auxiliary operations, such as the accelerator pedal control in cars and throttle lever control in aircraft. The value of n is determined by the length of the task profile. To ensure the practical applicability, subsequent analyses of timeliness and stability are calculated based on ***MCS***.
2) Calculate *HC_T*. Calculate *HC_T* under the task profile by:

$$HC\_T = T_j \left| \frac{MCS_j - MCS_{j+\Delta T}}{\Delta T} > k, j = 1, 2, \ldots, n \right. \quad (1)$$

where HC_T is the timeliness of ***MCS***, which is the position that satisfies the slope requirement change; T is the sequence unit of ***MCS***, also is the warning point of risk warning model, such as time, altitude, etc. k is the threshold of slop of ***MCS*** in ΔT, determined by the comprehensive human task profile and historical ***MCS***.

3) Calculate *HC_S*. Calculate HC_S under the task profile by:

$$HC\_S = \sqrt{\frac{1}{n-1}\sum_{j=1}^{n}\left(MCS_j - \overline{MCS}\right)^2} \quad (2)$$

where HC_S is the stability of ***MCS***; $\overline{MCS}$ is the mean of ***MCS***.

4) Calculate *HC_C*. Calculate HC_C under the task profile by:

$$HC\_C = \left| \left| HC\_T_{\mathrm{M}} - HC\_T_{\mathrm{A}} \right| - HC\_C_{\mathrm{SOP}} \right| \quad (3)$$

where HC_T_{M} and HC_T_{A} are the HC_T of ***MCS*** and ***ACS***; HC_C_{SOP} depending on the technology or management requirements controlled by humans.

5) Calculate HCM. Calculate HCM based on *HC_T, HC_S* and *HC_C*. Each *HC* is represented as a coordinate point in a three-dimensional space consisting of *HC_T, HC_S* and *HC_C*, where $HC = [HC\_T, HC\_S, HC\_C]$. The exploration of HCM can be conducted using a clustering-based approach, with *k*-Means clustering being a commonly used and effective method. Based on the classical *k*-Means clustering algorithm (Krishna & Murty, 1999), an analysis is conducted to identify several potential HCM that may exist within the current *HC*. The specific steps involved are as follows:

Step 1: Define the number of clusters *k*. The appropriate number of *k* is typically determined by practical requirements and the size of the *HC*. Additionally, to ensure the validity of the clustering results, we have set the sequence sample size for HCM clustering to be greater than 50 *k* based on empirical experience and removed outliers.

Step 2: Distance measurement. Assigning data points to the cluster with the nearest cluster center requires a nearest-neighbor distance measurement strategy. Since $HC = [HC\_T, HC\_S, HC\_C]$ represents points in a three-dimensional Euclidean space, the Euclidean distance metric is used to measure the distance between points. The calculation formula is as follows:

$$d(HC_1, HC_2) = \sqrt{\sum_{i=1}^{n}(HC_1, HC_2)^2} \quad (4)$$

Step 3: Calculation of new cluster centers $[HC\_T_c, HC\_S_c, HC\_C_c]_k$. For each of the *k* clusters generated after classification, calculate the point within the cluster that has the smallest average distance to other points. This point is then assigned as the new cluster center $[HC\_T_c, HC\_S_c, HC\_C_c]$. Continue this process iteratively to calculate the updated cluster centers.

Step 4: Determine if *k*-Means should stop. If the cluster centers no longer change or if the maximum number of iterations is reached, the process stops. At this point, the final set of cluster labels and their corresponding cluster centers $[HC\_T_c, HC\_S_c, HC\_C_c]_k$ represents HCM.

Step 5: The categories formed based on the cluster centers $[HC\_T_c, HC\_S_c, HC\_C_c]_k$ provide a basis for subsequent risk warning based on HCM. In practical applications across different domains, the identified HCM types can be assigned specific meanings and explanations. For example, an HCM characterized by early timeliness and good stability can be defined as conservative, while a late timeliness can be defined as adventurous. In other words, the category labels can be named and interpreted based on practical experience.

3.3. HCM-based real-time warning method for risk

In the current data-driven risk warning framework, traditional Safety-I models rely solely on risk data to construct warning methods, while Safety-II emphasizes the impact of risk evolution (Hollnagel, 2018). This study considers the influence of HCM on real-time risk warning. During real-time operations, the first step is to predict the HCM category currently employed by humans. Subsequently, risk warning is conducted based on the identified HCM. This section will provide explanations for both the data-based HCM analysis method and the risk warning method based on HCM. The following content outlines the methods for analyzing HCM based on data and conducting risk warnings based on HCM.

(1) HCM analysis method

HCM describes the control outcomes of humans over *HC_T, HC_S* and *HC_C*. Accurately identifying the factors that influence humans to exhibit different control modes is crucial for predicting HCM accurately. In order to extract relevant features from a data perspective, the analysis commences by adopting the "Human-Machine-Environment" perspective within the framework of a "human-in-loop" control system. With the human information processing process at its core—situation awareness, decision-making, and control—the data features are extracted as shown in Fig. 5.

As depicted in Fig. 5, the features used to construct the HCM analysis model can be classified into three categories: human factors, machine factors, and environmental factors. The human factors consist of situation awareness (SA), decision performance (DP), and task hardness (TH).

1) SA represents the ability of humans to perceive the current task environment. Its magnitude is influenced by factors such as

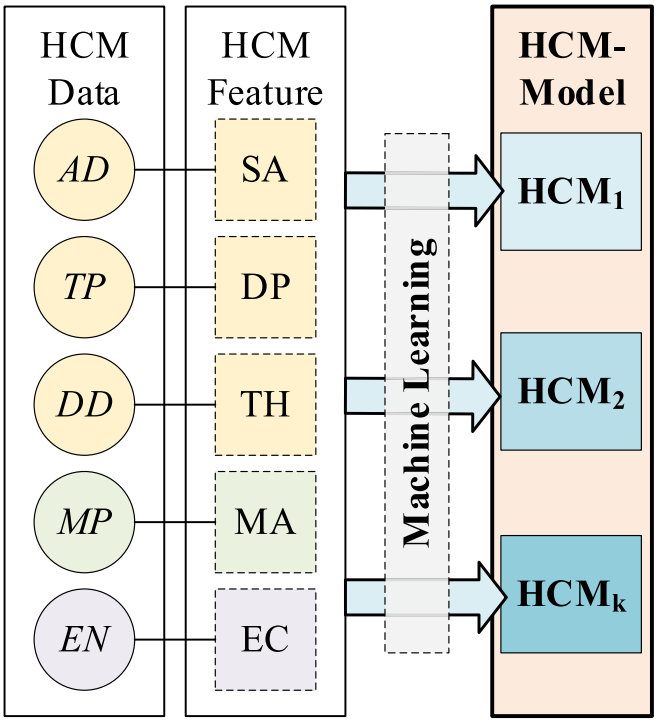

Fig. 5. Features and corresponding data for HCM analysis.

attention, physiological state, and psychological state (Endsley, 2021). SA directly affects the human capacity to gather information from the surrounding environment and may thus influence the resulting HCM. It is assumed that the deviation of man–machine system state can reflect the quality of human situational awareness (Zhirabok et al., 2018). Therefore, machine state deviations (*AD*), such as vehicle speed exceeding limits or aircraft airspeed exceeding limits, are used to measure the SA performance of humans. A larger *AD* indicates less accurate perception of the machine situation, while a smaller *AD* signifies more accurate perception.

2) DP measures how efficiently and accurately humans make decisions based on SA. It reflects the utilization of attentional resources, control knowledge, and control experience in making decisions regarding the current human–machine interaction. DP is eventually manifested in the performance of human–machine interaction tasks. In the study, parameters like trajectory stability in cars or aircraft track deviation (*TP*) are used to represent DP. A larger *TP* indicates less accurate perception of the machine situation, while a smaller *TP* signifies more accurate perception.
3) TH represents the complexity and difficulty of the current human–machine interaction task, which also reflects the level of risk in the system. Higher task hardness requires more demanding control decision-making and may also influence physiological and psychological states of humans, such as increased stress and fatigue. In the study, TH is characterized using a task degree of difficulty (*DD*), such as road bend radius or weather conditions

As shown in Fig. 5, *AD*, *TP*, *DD* are used to describe the SA and DP states of humans in the information processing process. *DD* is an important variable that influences decision-making and needs to be selected based on the profiles of human control tasks. Additionally, other machine factors (MA) and environmental condition factors (EC) serve as HCM features input into the machine learning process of human information processing, ultimately outputting HCM.

This study assumes that humans maintain a constant HCM within a certain task profile, meaning that individuals tend to choose a fixed control mode over a period of time. By using machine learning to simulate the human information processing process based on the aforementioned HCM features and corresponding HCM data, the study aims to predict HCM. The specific steps are illustrated in Fig. 6.

Step 1: Referencing the typical task process of the "human-in-loop" control system, collect a dataset D_{HCM} consisting of sequential data for HCM prediction, based on the task profile determined by the warning requirements.
Step 2: Calculate HCM based on the method proposed in section 3.2, which serves as the label for the D_{HCM}.
Step 3: Based on the warning requirements and the identified warning variables (*WV*), such as time and altitude, split the D_{HCM} dataset using the sampling frequency of *WV*. This is done to increase the sample size of the D_{HCM} dataset and improve the accuracy of D_{HCM} analysis based on machine learning, assuming a constant HCM within the task profile. A common data splitting process, as shown in Fig. 7, is used in this study, where the sequential data is divided into segments for HCM analysis based on *WV*.
Step 4: Calculate the data features as depicted in Fig. 5 and extract HCM analysis features and HCM labels from DHCM, forming a dataset D_{HCM}-ML for machine learning. In HCM feature calculation, the importance of features is analyzed based on the Gini coefficient from the random forest model, and the inter-feature correlation is assessed using the Pearson correlation coefficient.
Step 5: Utilize various types of machine learning models, such as Decision tree, Random Forest, XGBoost, LGBoost, on the D_{HCM}-ML. Compare the performance of these models and select the optimal model as the prediction model for HCM. The prediction accuracy *A*, precision *P*, recall *R* and comprehensive evaluation index F_1 are calculated to verify the availability of the HCM analysis model. The calculation formula of *A*, *P*, *R*, and F_1 is shown in formula (5):

$$\begin{cases} A = \dfrac{TP + TN}{TP + TN + FP + FN} \\ P = \dfrac{TP}{TP + FP} \\ R = \dfrac{TP}{P} \\ F_1 = \dfrac{2PR}{P + R} \end{cases} \tag{5}$$

where *TP* indicates that the positive class is predicted as positive class; *FP* means that the negative class is predicted as positive class; *A* indicates that the classification accuracy of all categories; *P* is the proportion of the real risk samples divided into corresponding risk labels; *R* means the classification accuracy rate of the actual risk samples; F_1 is the comprehensive evaluation index of the model.

(2) HCM-based approach to risk warning

Traditional data-based risk warning builds machine learning models based directly on risk outcome data, with little consideration of the impact of human control on risk labelling. After obtaining the human control model, it is necessary to synthesize the changes in machine motion and environmental states in the human–machine systems in real time to make more accurate judgements on risks. Unlike the assumption that the HCM is consistent across the task profile, there is uncertainty in the change of risk during the warning cycle, i.e., there are differences in the risk prediction model and prediction accuracy at different warning locations. The warning location has a significant impact on the change of system risk over the time-series, e.g., radio altitude is commonly used in civil aviation safety to provide risk alerts for take-off and landing processes. Further, risk alerting is also limited by the alerting mechanism, which includes the actual task requirements (e.g., the number of alerts) and the human's response time for emergency handling, and the real-time data transmission limitations, which include the data acquisition frequency and the data latency. In summary, the construction method of the risk warning model of the HCM-based human–machine systems is shown in Fig. 8.

Step 1: Select the warning points that trigger alerts $\{WP_1, WP_2, \ldots, WP_n\}$. The value of *n* is determined by the sampling frequency of *WP* and the desired recall rate of the final model.
Step 2: Choose the data slicing range $\Delta WP = (WP_{max}\text{-}WP_{min})/n$ and construct the risk alert dataset $\boldsymbol{DW} = \{\boldsymbol{DW} - \boldsymbol{S}_i\}\ i = 1,2,\ldots,n$, for machine learning training.
Step 3: Within each data slice $\boldsymbol{DW} - \boldsymbol{S}_i$, group the $\boldsymbol{DW} - \boldsymbol{S}_i$ based on the predicted results of HCM, forming the ***DW-S***-HCM dataset.

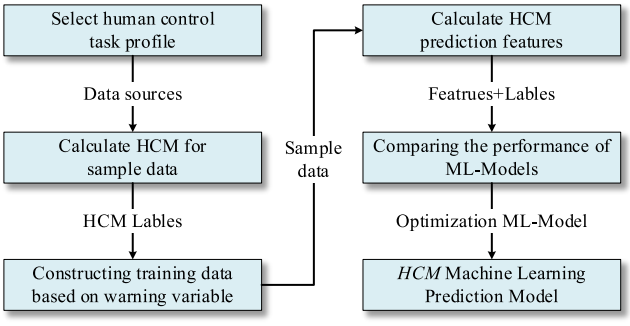

Fig. 6. HCM analysis steps.

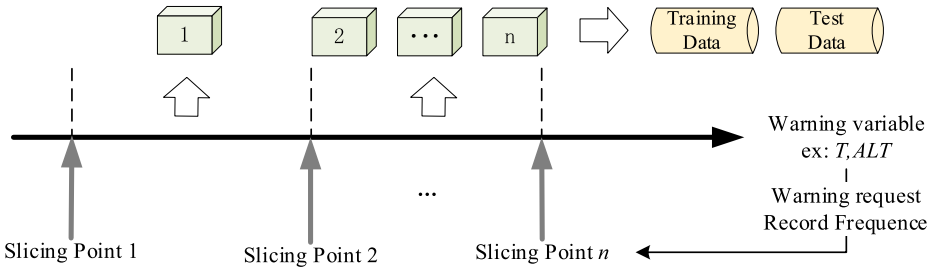

Fig. 7. Data segmentation.

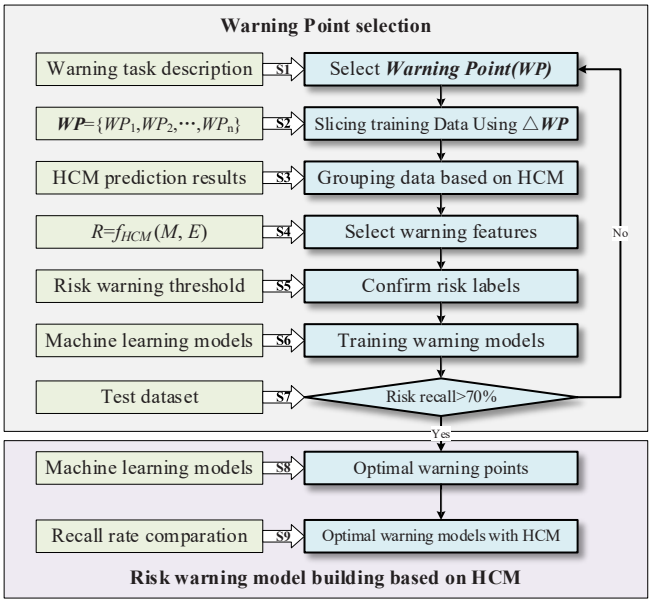

Fig. 8. Risk warning method based on HCM.

Step 4: Referencing the disciplinary equations of the human–machine system, select machine state parameters and environmental change parameters as features for risk prediction.
Step 5: Set the risk labels based on typical risks in the human–machine environment and corresponding risk management thresholds.
Step 6: Train machine learning models within ***DW-S***-HCM and calculate the average risk recall rate $\boldsymbol{DW}-\boldsymbol{S}_i$ of each model on the test data.
Step 7: Select the optimal ΔWP, ensuring that the corresponding $\boldsymbol{DW}-\boldsymbol{S}_i$ of $R_{\text{DW-S}}$ is above 70 %.
Step 8: Train machine learning models at the optimal warning position corresponding to ΔWP.
Step 9: Select the machine learning model with the highest risk recall rate to construct the optimal real-time risk warning based on HCM.

4. Case study

The case study focuses on aviation industry, specifically examining the impact of pilot HCM on flight accidents. Among them, the aircraft approach and landing phase is a high-risk stage for flight accidents. Currently, aircraft landing has not been fully automated and relies mainly on manual control by pilots. Improper pilot control may induce unsafe events such as hard landings, long landings, and tail strikes (Tong et al., 2018; Wang, Wu, & Sun, 2013; Wang et al., 2018). This system is a typical "human-in-loop" control system with high risk. To ensure an acceptable level of flight safety, it is urgently needed to develop effective risk warning methods based on flight data, focusing on HCM.

The case study focuses on the real-time risk warning based on flight data and human control for the two typical landing risks: hard landing and long landing, which could do risk warning by flight data by machine learning (Xiangzhang et al., 2024; Zhang et al., 2023). Flight risk warning relies on real-time air-ground data transmission technologies, including Automatic Dependent Surveillance-Broadcast (ADS-B), Communication, Navigation, Surveillance / Air Traffic Management Datalink (CNS/ATM Datalink), On-Board Avionic Networking System (OANS), Very High Frequency (VHF) radio communications, and satellite communications, etc. Currently, the Quick Access Recorder (QAR) data is an important foundation for aircraft state estimation and safety assessment (Wang, Wu, & Sun, 2014), which includes pilot control data. Therefore, the case study uses QAR data for feasibility verification of the method, without considering the impact of air-ground data transmission technologies on the warning effectiveness.

4.1. Selection of parameters for aircraft landing risk warning

The landing risk of an aircraft is the result of the combined effects of human control, machine state, and environmental changes. To accurately obtain the warning parameters for landing risk, relevant variables can be obtained from the perspective of the underlying physical laws of the aircraft landing system, thereby guiding the selection of risk warning parameters.

(1) Parameters for Hard Landing warning

Hard landing is a physical phenomenon that occurs when an aircraft makes contact with the ground during landing, characterized by excessive longitudinal acceleration. Taking symmetric landing, where the main landing gears touch the ground simultaneously, as an example, the parameters for hard landing risk warning are analyzed.

As shown in Fig. 9 and Fig. 10, in the two-point grounding, i.e., the main landing gear grounding phase, the equations of motion can be described as:

$$m\dot{z} = -2F_{s\_m}\cos\alpha + W \tag{6}$$

$$W = mg - \frac{1}{2}\rho S(V - V_{\text{W}})^2 C_{\text{L}} \tag{7}$$

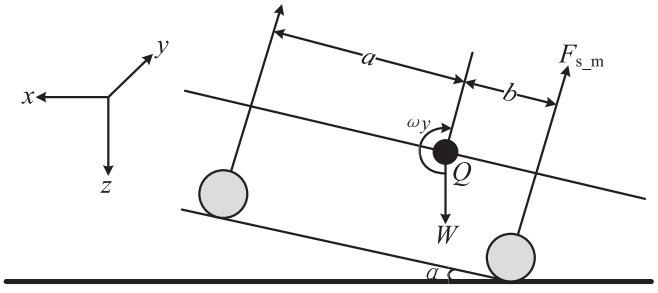

Fig. 9. Side view of aircraft landing.

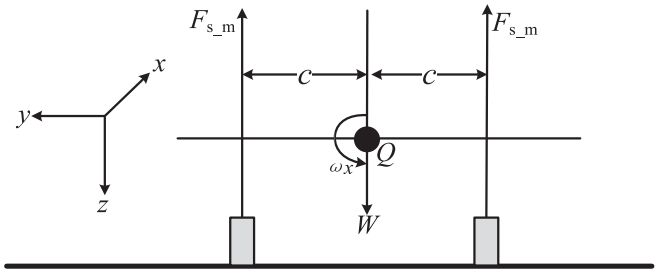

Fig. 10. Front view of aircraft landing.

$$I_y\dot{\omega}_y = -2bF_{s\_m} \tag{8}$$

$$I_x\dot{\omega}_x = -2cF_{s\_m}\cos\alpha \tag{9}$$

where m is the aircraft gross weight; $\dot{z}$ is vertical acceleration of aircraft; F_{s_m} is the impact force of the main landing gear on the fuselage of an aircraft; α is the angle between the aircraft fuselage reference line and the ground is called the pitch angle; W is the equivalent weight of the aircraft, including comprehensive lift; g is the gravitational acceleration; ρ is the atmospheric density; S is the wing reference area; V is the touchdown speed; V_W is the vertical wind speed (headwind is positive); C_L is the lift coefficient; I_y is the moment of inertia of an aircraft around its horizontal axis; I_x is the moment of inertia of an aircraft around its longitudinal axis; $\dot{\omega}_y$ and $\dot{\omega}_x$ is the angular acceleration of the aircraft's rotational motion around the horizontal axis and the vertical axis, respectively; b is the distance from the longitudinal axis to the center of gravity at the connection point between the main landing gear and the fuselage of the aircraft; c is the distance from the horizontal axis to the center of gravity at the connection point between the main landing gear and the fuselage of the aircraft.

It can be seen that excessive $\dot{z}$ will cause a hard landing of the main landing gear, that is, the vertical descent rate of the aircraft is too high, resulting in excessive ground forces on the main landing gear, and thus an excessive impact force on the fuselage. At the same time, during the three-point touchdown phase, if the rate of change in pitch angle is too large, the F_{s_n} acting on the fuselage by the front landing gear will also be too large when the front landing gear touches down, causing a hard landing of the front landing gear. The pilot's HCM is the direct cause of the change in pitch angle. Meanwhile, the uncertain changes in V_W can also cause fluctuations in $\dot{z}$, such as wind shear. The changes in other parameters during the grounding phase are relatively small and will not be considered temporarily.

(2) Parameters for Long Landing warning

Aircraft landing refers to the process of descending, touchdown, rolling, and ultimately coming to a stop on the runway, starting from a height of 50 ft above the threshold of the runway. The landing phase is typically divided into three stages: the descent and flare phase, the transition phase, and the deceleration and rollout phase, as depicted in Fig. 11.

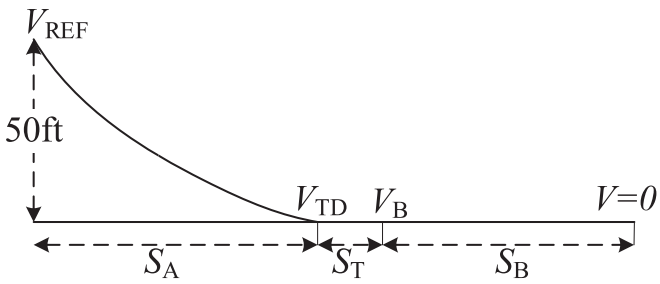

Fig. 11. Schematic diagram of aircraft landing phase.

Long landing refers to the situation where an aircraft utilizes a runway length that is excessive, which can lead to an runway overrun. The physical principles behind long landing can be illustrated using the descent and S_A an example. Prior to formally entering the landing phase, the aircraft remains on the approach glide slope. The phase in which the aircraft transitions from the glide path to the flare is known as the descent and flare phase. During this phase, the aircraft's throttle is set to idle, and it descends at a glide angle of 3° with V_{REF}. This process can be further divided into a straight descent segment and a flare arc segment. In the straight descent segment, the aircraft can be approximated as undergoing a constant descent with a glide angle of 3° and a velocity of V_{REF}. In the flare arc segment, the aircraft is assumed to maneuver along a circular arc with a radius of R, as depicted in Fig. 12.

The dynamic analysis of this process is as follows:

$$S_A = \frac{H_{LK}}{\theta} + R\frac{\theta}{2} \tag{10}$$

where H_{LK} is the vertical altitude at which the aircraft passes through the runway threshold; θ is the sliding angle, $\tan\theta \approx \sin\theta = \frac{D-P}{W}$; R is the radius of flare control, $R = \frac{W}{S_W}\frac{2n}{\rho C_L}\frac{1}{g(n-1)}$; S_A is the horizontal distance of the sliding and leveling section:

$$S_A = \frac{H_{LK}}{\left(\frac{C_D}{C_L} - \frac{P}{W}\right)} + \frac{\frac{W}{S_W}\left(\frac{C_D}{C_L} - \frac{P}{W}\right)}{\rho g(n-1)C_L} \tag{11}$$

The analysis of the various landing motion equations discussed above is based on the assumption of rigid body aircraft, neglecting the elastic deformation of the aircraft at the moment of landing. Through an analysis based on physical principles, it is evident that parameters such as landing weight, longitudinal acceleration, descent rate, pitch angle, roll angle, lateral acceleration, longitudinal wind speed, and their interrelationships truly reflect the actual conditions of aircraft landing, serving as the primary warning parameters for aircraft landing. Among them, the uncertainty of the pitch angle and roll angle is influenced by HCM. Additionally, the variability of wind speed introduces uncertainty, making it challenging to derive precise results for warning based on physical principles.

Therefore, this study takes a data science approach, quantifying the pilot's HCM based on historical flight data and training machine learning models with strong time-series prediction capabilities to achieve accurate warning of aircraft hard landings. Integrating the aforementioned equation analysis and the variables that can be recorded by the Quick Access Recorder (QAR) data of the B737-800 aircraft, aircraft risk warning parameters are selected from "Human-Machine-Environment" perspective, with the current QAR sampling frequency set at 1 Hz.

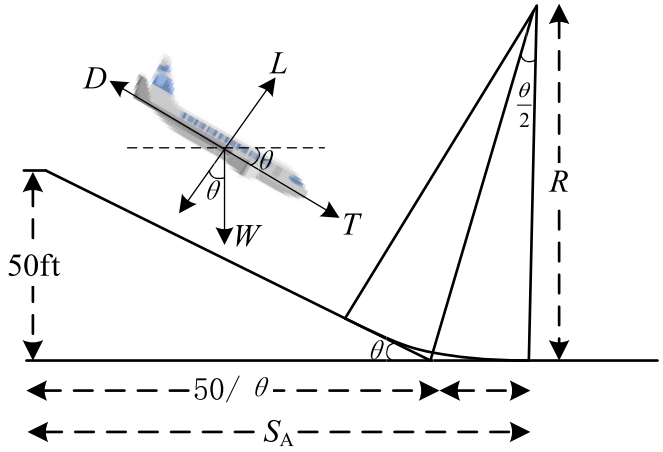

Fig. 12. Schematic diagram of aircraft approach and leveling phase.

The final selection of QAR parameters is presented in Table 1.

4.2. Pilot HCM mining

The case study considers the pilot's column control as the main control (*MC*) and the throttle control as the auxiliary control (*AC*), calculates the timeliness, stability and coordination using ***MCS*** and ***ACS***, and identifies typical pilot HCM based on clustering. Since aviation mostly use altitude as the reference variable, the Fig. 13 and Fig. 14 shows the changes of ***MCS*** and ***ACS*** within the current QAR data during the landing phase (50 ft-0 ft), and the subsequent risk warnings will use altitude as the reference variable for the warning point as well.

Referring to the B737-800 SOP (Academia, 2024)for landing operation, the pilot enters the landing operation after reaching V_{REF} at 50ft, and pulls the stick smoothly and continuously by throttling down in order to ground the aircraft. The SOP suggests that the pilot adopts a timely and smooth landing operation, and suggests that pulling the control column and throttle column down should be started at the same time, which means $HC\_C_{SOP} = 0$ in formula (3). Thus, according to SOP, the *C_T, HC_S* and *HC_C* of ***MCS*** and ***ACS*** may directly affect the evolution of the flight risk and the outcome of the risk warning.

However, as shown in Fig. 13 and Fig. 14, it can be seen that there are situations where the operations taken by the pilots do not fully comply with the SOP, i.e., there are problems such as untimely operation, poor stability, or lack of co-ordination that may become potential factors for inducing risks. From the physical equations in 4.1, it can be seen that the pilot's control directly affects the change of the aircraft's motion in the horizontal and vertical directions. Therefore, the altitude in flare is chosen to characterize *HC_T*, the control column fluctuation after flare is chosen to characterize *HC_S*, and the gap between the stick pull operation and the throttle retract operation is chosen to characterize *HC_C*, which were calculated based on Eqs. (1)–(3). The Fig. 15 show the statistical distribution of the above three parameters in the landing phase, respectively.

Further the data were analyzed by *k*-Means with *HC_T*, *HC_S* and *HC_C* as the three-dimensional spatial coordinates, and the results are shown in Fig. 16.

The *k*-Means clustering results indicate that there are three types of HCM for the pilots represented by control data, which are defined based on practical experience in civil aviation safety, such as Flight Crew Operation Manual (Skybrary, 2024), in order to make them easier to understand for safety managers. The individual HCM labels were defined as SOP, Conservative and Adventurous from the clustering centers and their corresponding coordinates, as shown in Table 2.

From Table 2, it can be seen that the three types of control modes represented by HCM differ in *HC_T*, *HC_S* and *HC_C*, reflecting the three types of different control strategies of different pilots in the past landing control process, and whether these three types of HCM affect the risk evolution needs to be analyzed in the context of a specific risk warning model.

Table 1
Parameters affecting HCM and risk in aircraft landing safety.

Classification	Symbol	Description
Human Control (*HC*)	*MC*	The angle of control column deviated from original point
	AC	The angle of thrust column deviated from original point
Aircraft Performance (*AP*)	*m*	Gross weight of aircraft
	ALT	The altitude of an aircraft relative to the ground
	V_A	The speed of aircraft indicated by instrument
	V_{REF}	The reference speed of aircraft in Landing
	FLAP	The setting position of flap handle
	LG	The position of landing gear
	IVV	The aircraft descent rate
	VRTG	The vertical acceleration of aircraft
	PITCH	The pitch of aircraft
	ROLL	The roll of aircraft
	GD	The glide slope deviation of the aircraft
Environment (*EN*)	V_W	The wind speed along the longitudinal axis of the aircraft
	P_S	The static pressure of air
	T_S	The static temperature of air
	ρ	The density of air, calculated by $\rho = \frac{P_S}{RT_S}$,where R = 287.15 J/(kg·k)

4.3. Machine learning based real-time warning of risks

After mining the pilot HCM in the historical flight data, they are applied in the real-time warning of aircraft landing risk. Firstly, it is necessary to judge the HCM adopted by the current pilot based on the real-time data, and then to warn the landing risk of the current HCM based on the real-time data.

(1) Pilot HCM analysis and prediction

Pilot switches off autopilot and starts manual control at about 1300ft, so analysis of pilot HCM is based on the data between 1300ft-50ft. The general aircraft descent rate is about 3 m/s, that is, the pilot takes over the aircraft at 1300f and starts landing at 50 ft after about 2 min. Therefore, we assuming that the pilot HCM selected by the pilot during the period of 1300 ft-50 ft remains unchanged from 50 ft-0 ft during the landing phase (which lasts for about 5 s or so). Then, as shown in Fig. 17, the historical high-dimensional sequence data can be sliced based on altitude according to the altitude to obtain sample data for constructing the pilot HCM prediction model.

During the landing process, the pilot uses various parameters to judge the control mode adopted. For the control process of the landing process, based on the results of the analysis of the human factors in 3.3 and the results of the analysis of the equations in 4.1, the QAR parameters selected for the prediction of the pilot HCM are shown in Fig. 18.

Based on the samples constructed from the sliced data and the HCM warning features, the machine learning-based HCM analysis model is constructed, and the performance results of its performance on the test dataset are as in Table 3:

As can be seen from Table 3, DT has the best overall performance for HCM, and all performance indicators are higher than 90 %, so DT is chosen as the HCM analysis model for real-time warning of aircraft landing risk, which is used to subsequently make more accurate warning of the risk of landing accidents brought about by different HCM.

(2) HCM-based risk warning for flight landing accidents

Further predictions of typical aircraft landing risks were made based on the acquisition of HCM. The flight landing risk warning risk labels used for the case study include: Safety (S), hard landing (H), long landing (L), hard landing and long landing (H&L). Based on the parameter selection in 4.1 and the current airline judgement criteria for hard landing and long landing, the landing risk prediction characteristics and risk labels used are given as shown in Table 4.

Selecting an appropriate machine learning model for risk prediction is the core of flight landing risk warning, and the performance of the machine learning model is limited by the number of samples in each risk category, which is affected by the combined effect of data collection frequency and *WP*. The current landing radio altitude warning interval for civil airliners is 100ft, and the data between 100ft and 200ft, i.e., $\Delta WP = 100$ft, is used as an example to train the risk warning machine learning models for different HCM, and the results are shown in Fig. 19.

Preliminarily, from the Fig. 19, at $\Delta WP = 100$ft:

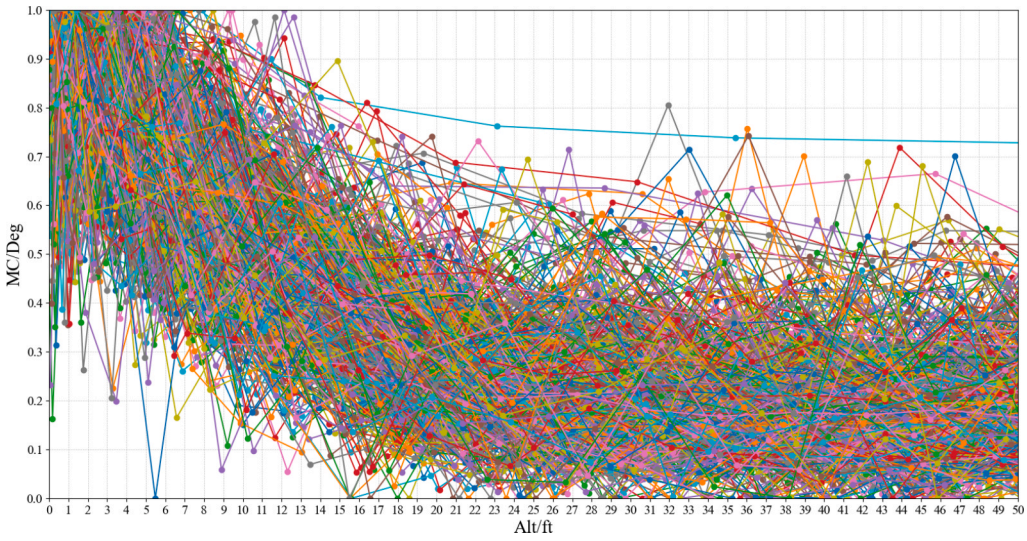

Fig. 13. *MC* in aircraft landing stage.

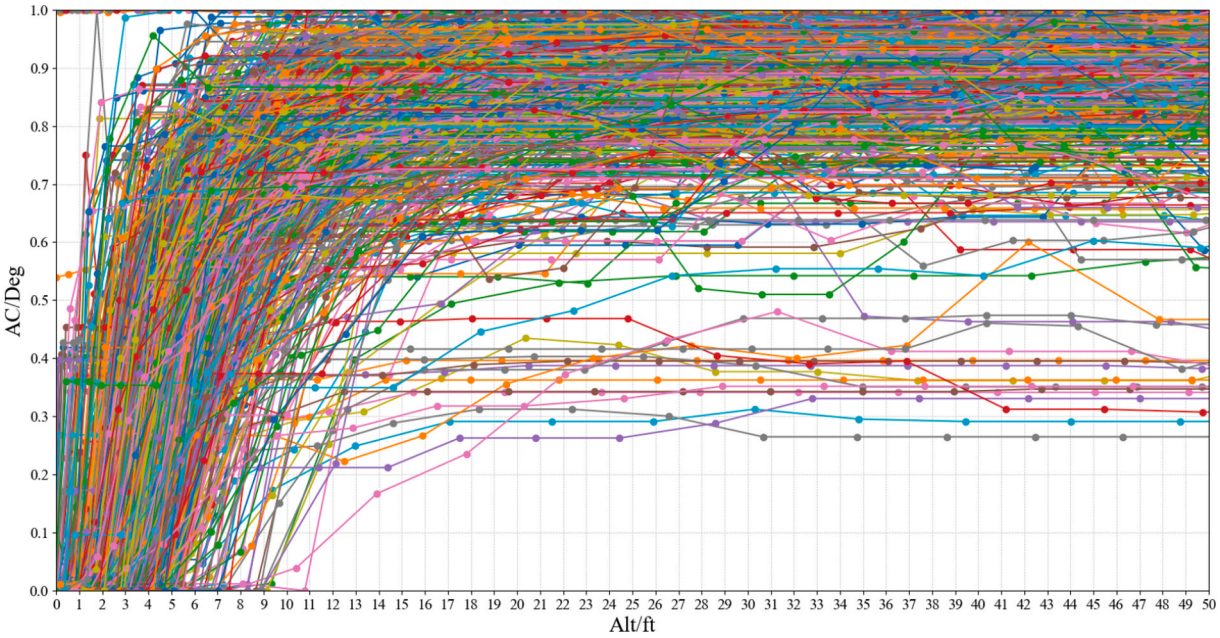

Fig. 14. *AC* in aircraft landing stage.

1) the mean recall for H, L and H&L is higher in the HCM group than in the no HCM group;
2) the recall rates for the H, S, and L risk categories within each HCM group are greater than 60 %, providing risk warning significance.
3) H&L within each HCM group could not achieve a satisfactory recall rate.
4) There are differences in the prediction performance of different machine learning for risks other than category S.

As can be seen, before considering which machine learning model to use, the ΔWP needs to be selected reasonably so that the warning model can have a high recall for all types of risks. Therefore, the recall of the model at different warning heights needs to be further explored, especially for risk categories such as H&L, where the sample proportion is small. Based on the processing in Fig. 20 to obtain data slices corresponding to the radio altitude, the average recall of the machine learning model under different ΔWP is explored for the H&L class, which is currently the worst classified class.

As shown in Fig. 21, different ΔWPs are selected to set the warning points in the range of 1300ft-50ft to further explore the recall of the model for H&L under different warning point configurations and find the optimal warning points.

As can be seen from Fig. 21:

1) As ΔWP increases, it makes the machine learning model's recall for H&L increase due to the increase in the number of samples;
2) After the warning interval is higher than 200ft, the recall of the machine learning model for the H&L class starts to be higher than 50 %;
3) The warning point after ΔWP is higher than 400ft meets the actual warning needs, i.e., 2–3 warnings are performed.

Comprehensive H&L recall rate and to achieve effective warning to pilots, the selected warning altitude interval is 400ft, i.e., three landing

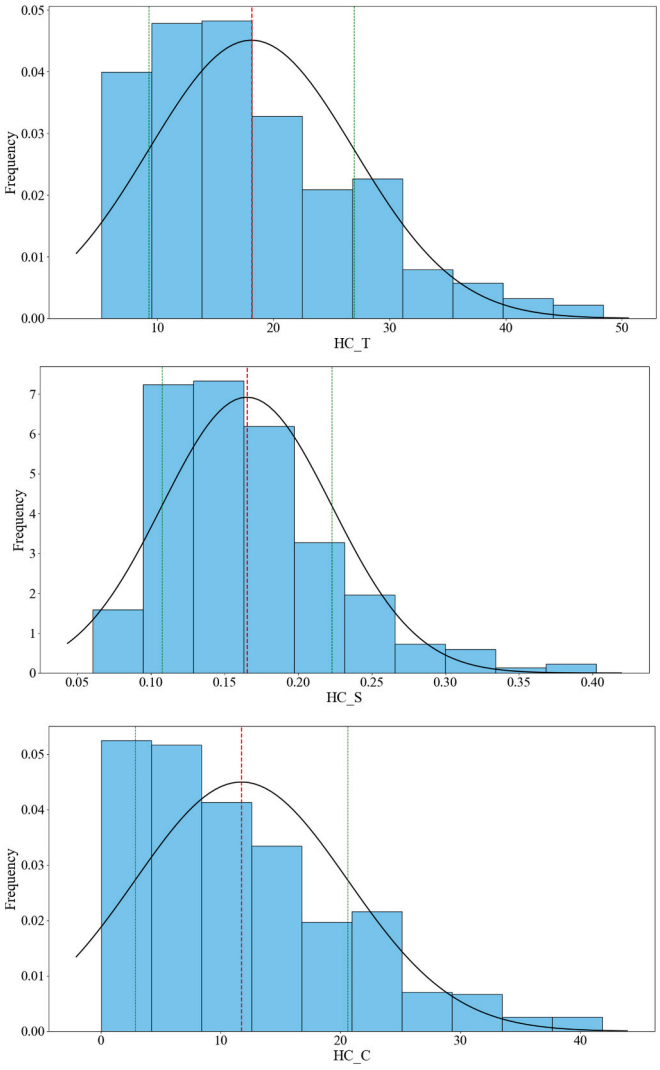

Fig. 15. Frequency histograms of HC-T, HC-S, and HC-C.

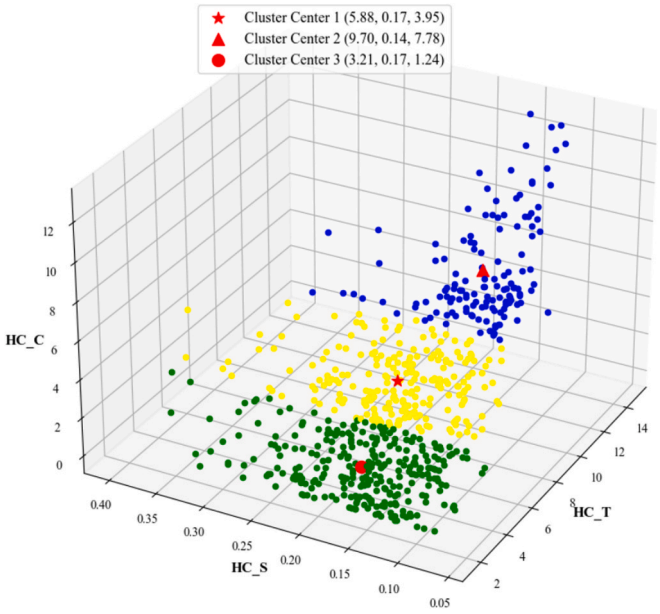

Fig. 16. Results of HCM by *k*-Means.

Table 2
HCM label illustration.

HCM Label	Cluster center	HCM explain	HCM
SOP	[19.29, 0.17, 12.95]	The flare height is moderate, the control is stable, and the control coordination is moderate	Timely, stable, and coordinated control
CON	[31.82, 0.14, 25.52]	The flare height is high, the control is very stable, and the coordination of control is weak	Control early, very stable, and uncoordinated
ADV	[10.53, 0.17, 4.06]	The flare height is low, the control is stable, and the control coordination is great	Late control, stable, and well-coordinated

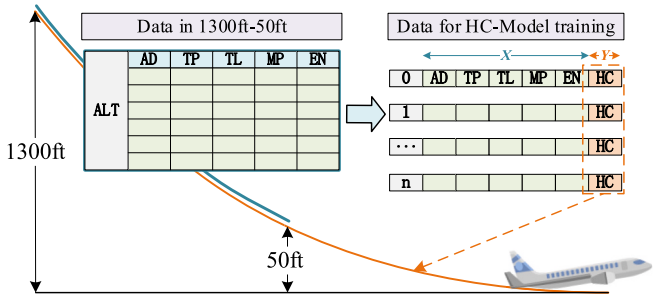

Fig. 17. Altitude-based data slicing for HCM analysis.

risk warnings are conducted at 100ft, 500ft and 900ft, and the machine learning models selected for each warning location and HCM and the comprehensive performance (average recall rate of each risk category) are shown in Table 5.

As can be seen from Table 5:

1) the machine learning models in the HCM group have high prediction accuracy for landing risk;
2) The average recall rate of machine learning models can be generally lower than that of the HCM group when HCM is not considered;
3) Different HCM of different *WPs* correspond to different machine learning models.

In the actual prediction process, it is necessary to judge the HCM before risk prediction. Therefore, the prediction model of HCM and the corresponding risk prediction model together determine the performance of the HCM-based risk warning model. Based on the recall of the HCM analysis model using DT in Section 4.2, the performance of the final HCM −based risk warning model is calculated as shown in Fig. 22.

From the table, it can be seen that the early warning model can recall more risk samples after considering HCM, and for risk warning, a difference of 1 % may mean serious accident consequences. Therefore, risk prediction based on HCM has important practical significance. Eventually, the recall rate of each HCM for various types of risk labels at different warning positions is shown in Fig. 23.

As can be seen from Fig. 23:

1) the recall of each HCM model for safe samples is close to each other, while there is a difference in the recall for risky samples, with the lowest recall for H&L;
2) For the same warning location, the SOP and ADV models have higher recalls, and the CON has a slightly lower recall;
3) for different warning positions, 500ft has the highest recall across HCM models.

5. Discussion and future work

In order to improve the accuracy of real-time risk warning methods,

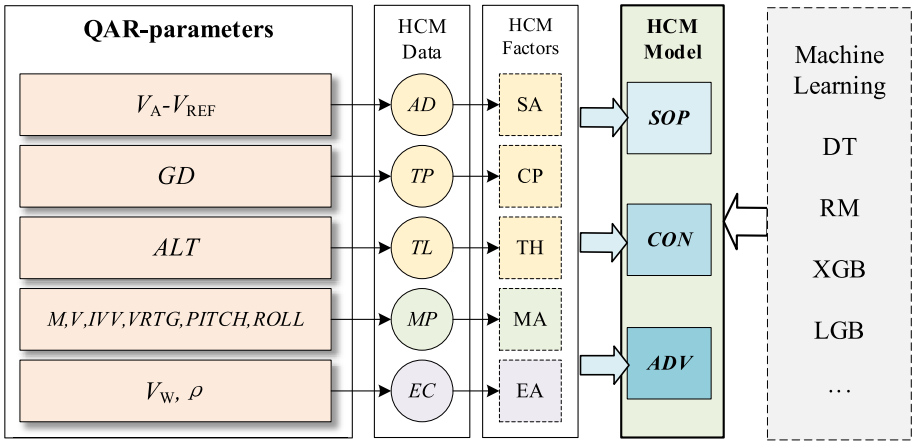

Fig. 18. HCM prediction features and machine learning model selection.

Table 3
Comparison of HCM prediction model performance.

ML-Model	HCM	Precision	Recall	F1-score	Accuracy
DT	SOP	0.95	0.97	0.95	**0.95**
	CON	0.95	0.93	0.94	
	ADV	0.96	0.96	0.96	
RM	SOP	0.93	0.98	0.96	0.93
	CON	0.99	**0.89**	0.93	
	ADV	0.93	0.98	0.96	
XGBOOST	SOP	0.95	0.99	0.97	0.95
	CON	0.95	**0.86**	0.90	
	ADV	0.92	0.96	0.94	
LightGBM	SOP	**0.88**	**0.89**	**0.88**	0.88
	CON	0.96	**0.74**	**0.84**	
	ADV	**0.86**	0.94	0.90	

Table 4
Features of Aircraft Landing Risk warning and Explanation of Risk Labels.

Risk warning features ***X***	Labels ***Y***	Label content	Determination parameters	Label determination rules
V_A, V_W, ρ, *IVV*, *VRTG*, *PITCH*, *ROLL*, *SD*	S	No risk	\	\
	H	Hard landing	*VRTG*	*VRTG* > 1.6 g
	L	Long landing	S_A	S_A > 800 m
	H&L	Hard and long landing	*VRTG* &S_A	*VRTG* > 1.6 g &S_A

human control is considered as a key mechanism influencing the real-time risk evolution of human–machine systems. The research is discussed as follows:

(1) HCM mining

The "timeliness", "stability" and "coordination" in the HCM mining method are directly derived from human control sequences, including main control and auxiliary control, to achieve the objective features of human–machine interaction. In the flight safety scenario, three types of typical pilots were identified based on "timeliness", "stability" and "coordination" through k-Means, which were named as SOP, CON and ADV. Among them, CON tends to control early and smoothly, but with poor coordination; ADV tends to control late and coordinately, but with poor stability; SOP is more in line with the recommendation of flight control, i.e., timely control with stability and coordination. The results of the performance evaluation of HCM-based risk real-time warning model further indicate that HCM has an impact on the warning results of the risk, suggesting that mining the HCM has research and application value at human–machine systems risk management. However, the interpretability of HCM labels needs to be further studied through human factors experiments or questionnaires.

(2) "Human-Machine-Environment" orientated HCM analysis

In order to obtain an accurate HCM in the risk real-time warning process, the features affecting the HCM are analyzed based on the human information processing model, and concludes that the HCM is the result of human information processing and is affected by human situational awareness, decision-making performance, task difficulty, and a combination of machine state and environmental conditions. However, this deterministic approach may overlook emergent cognitive dynamics (Flach, 1995). Future iterations may integrate Ecological Interface Design principles to better support situated decision-making (Rasmussen, 1999). In the flight safety scenario, a pilot HCM analysis model with an accuracy of up to 95 % is obtained based on the decision tree algorithm to support the realization of accurate real-time risk warning. After the risk warning model integrates the accuracy of HCM analysis, it finally achieves a risk recall rate as high as 85 %, which is higher than the risk warning model without considering HCM, and thus has great practical significance at the human–machine systems risk prevention.

(3) HCM-based risk warning

The study concludes that the selection of warning points affects the accuracy of the HCM-based risk warning model, and proposes a method for selecting warning points based on warning demand and data transmission frequency. In the flight landing risk warning scenario, three warning points are finally selected at the altitudes of 100ft, 500ft and 900ft. Meanwhile, the machine learning models selected for different HCM risk warning models at different warning points are different. The final result shows that the recall rates of the risk warning model at the three altitudes of 100ft, 500ft and 900ft meet the requirements for use, in which the scheme has the highest risk recall rate at 500ft, and the CON group and SOP group have higher risk recall rates at the three warning points. The above results show the importance of the reasonable selection of warning points and the effectiveness of building HCM-based risk warning model.

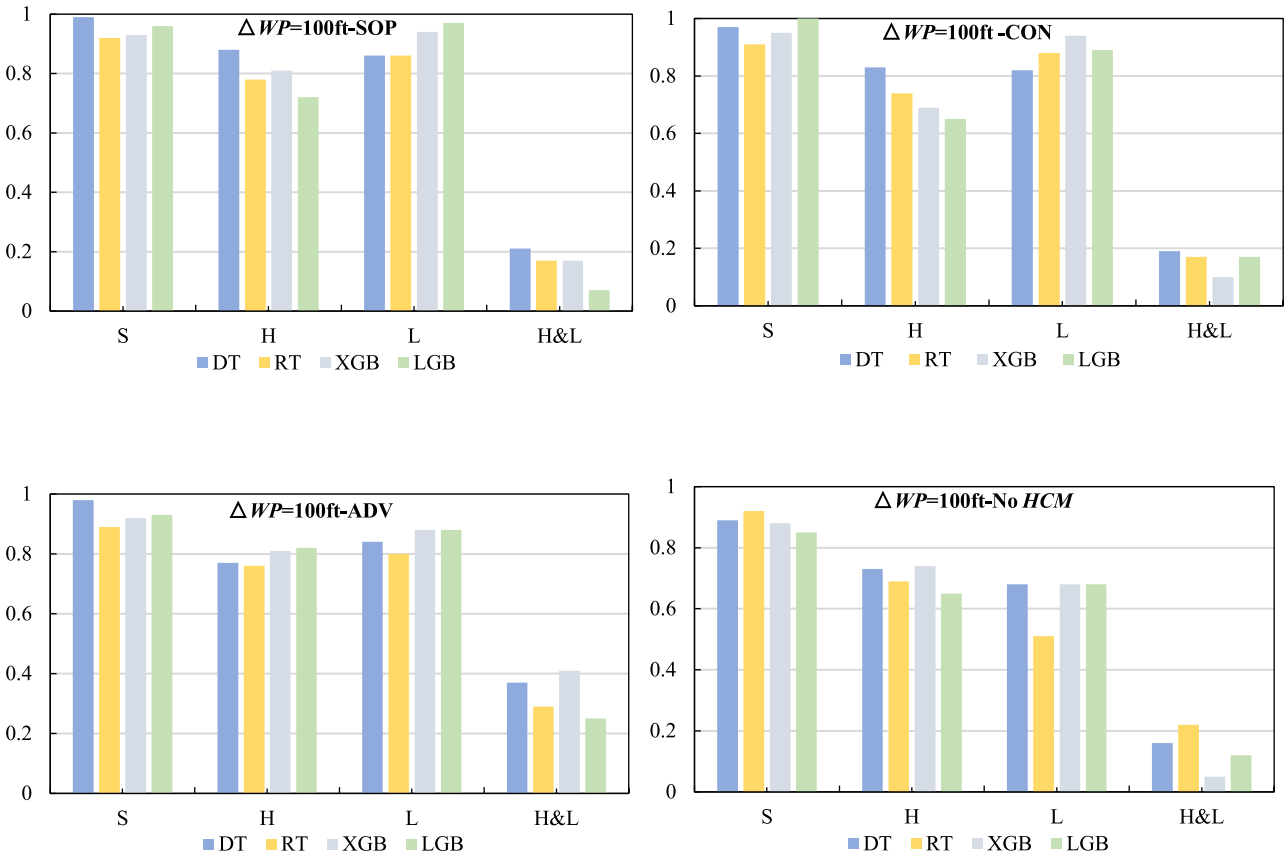

Fig. 19. Comparison of recall rates for various risks using machine learning models with $\Delta WP = 100$ft.

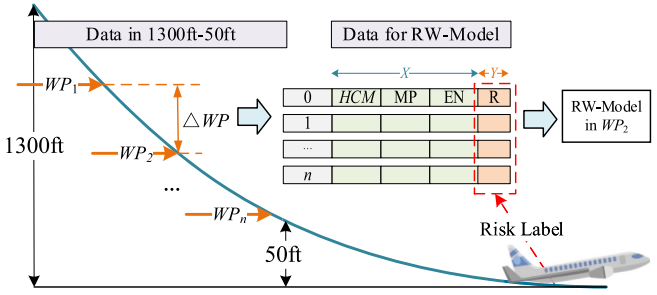

Fig. 20. Height based data slicing for risk warning based on HCM.

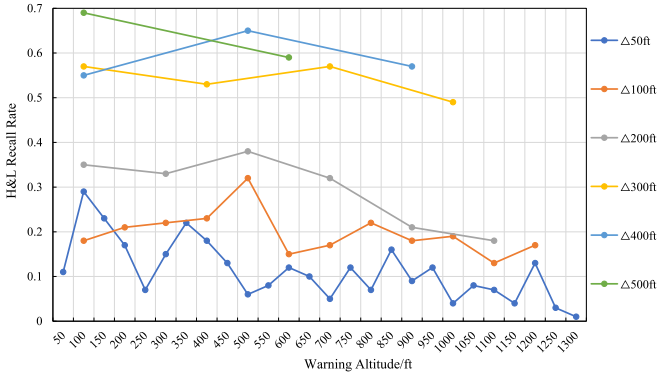

Fig. 21. Risk H&L recall rates for different warning altitude intervals.

Table 5
Recall rates and selected machine learning models for various heights under the Δ400 warning standard.

WP	HCM	ML-Model	Mean Recall
900ft	SOP	LGB	0.84
	CON	LGB	0.83
	ADV	DT	0.85
	No HC	DT	0.77
500ft	SOP	XGB	0.90
	CON	LGB	0.87
	ADV	XGB	0.92
	No HC	XGB	0.80
100ft	SOP	XGB	0.88
	CON	LGB	0.85
	ADV	LGB	0.88
	No HC	LGB	0.79

(4) Future study

In future research, HCM can be considered to be extracted from richer data, such as video data and audio data, or more clustering methods, such as density-based clustering, probability-based clustering, and sequence-based clustering, can be used to mine richer HCM expressions. Meanwhile, further research on the interpretable model of HCM is needed to identify the human cognitive factors and structures affecting HCM, such as attention, situational awareness, fatigue, and stress, etc., and to find the accurate representations of the above human factors on control data through physiological-psychological experiments.

For the research of real-time risk warning, firstly, it is necessary to

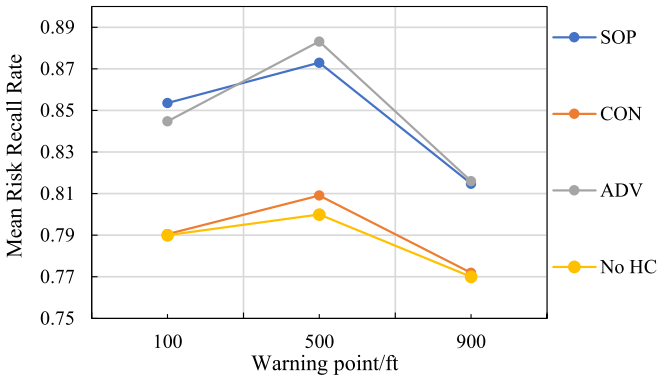

Fig. 22. Comparison of Model Performance for Different Warning Altitude Positions.

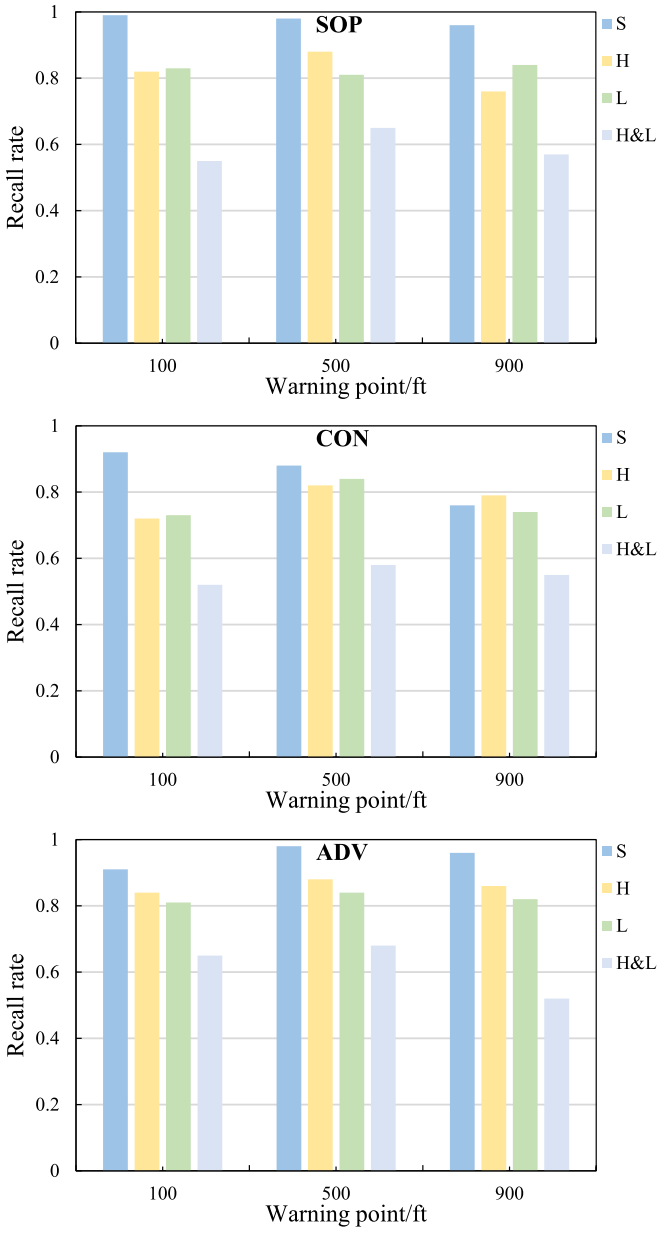

Fig. 23. Comparison of performance in warning point of Risk warning model based on HCM.

explore the influence mechanism of HCM on specific risk types based on the consideration of HCM, for example, pay more attention to the change of SA in the process of real-time dynamic interaction between human and machine, so as to prompt the effectiveness of early warning (Wen et al., 2023); secondly, it is necessary to further strengthen the data coverage and transmission rate from the perspective of sub-risk management, in which the data coverage solves the problem of covering various types of uncertain risks and reduces the data imbalance; The transmission rate solves the real-time problem of warning, especially the collection of various human control data is used to achieve real-time analyses of human control status, however, such analyses need to pay attention to the ethical and privacy issues in the application process.

While case study focuses on aviation, the methods developed can be extended to other industries relying on Human-Machine Interfaces and Supervisory Control and Data Acquisition (SCADA) systems. By integrating human behavior and machine state data, the approach can enhance real-time monitoring and predictive analytics in sectors like manufacturing. This could help prevent equipment failures and operational anomalies, improving safety and efficiency. Future work will explore these applications, demonstrating the broad potential of human-centric risk warnings across various domains.

6. Conclusion

Human control is regarded as an essential driver in the dynamic progression of real-time risk within human–machine systems. In order to solve the problem of the influence of human control on risk warning, this study proposes a real-time risk warning method based on HCM. The method takes human control sequences as the core, calculates the features of sequences from three dimensions of “timeliness”, “stability” and “coordination”, and uses clustering method to derive typical HCM. On the basis of precise HCM prediction based on human information processing model, the HCM is used to achieve more accurate risk warning. The proposed methodology is applicable to typical flight landing risk warning scenarios, and is useful for improving data-driven flight safety management and reducing risks in other similar areas. Meanwhile, in the context of the current lack of research on human factor mechanisms, HCM-based risk warning at the data-driven level has a wide range of industry applications, which emphasizes risk control in human–machine systems.

CRediT authorship contribution statement

Chongfeng Li: Writing – review & editing, Writing – original draft, Visualization, Validation, Software, Resources, Methodology, Formal analysis, Data curation, Conceptualization. **Xing Pan:** Supervision, Project administration, Methodology, Funding acquisition, Conceptualization. **Linchao Yang:** Supervision, Software, Resources, Project administration, Funding acquisition. **Jun Wang:** Resources, Project administration, Funding acquisition. **Haobing Ma:** Writing – review & editing, Visualization, Software.

Acknowledgement

This work is supported by the National Natural Science Foundation of China under Grant No. 72071011.

Data availability

The authors do not have permission to share data.

References

Academia, 2024. Boeing 737-800 standard operations procedure.

Aziz, S., & Dowling, M. (2019). Machine learning and AI for risk management. In *Disrupting finance: FinTech strategy in the 21st century* (pp. 33–50).
Bertoncel, T., Erenda, I., Bach, M. P., Roblek, V., & Meško, M. (2018). A managerial early warning system at a smart factory: An intuitive decision-making perspective. *Systems Research Behavioral Science, 35*, 406–416.
Bury, T. M., Sujith, R., Pavithran, I., Scheffer, M., Lenton, T. M., Anand, M., & Bauch, C. T. (2021). Deep learning for early warning signals of tipping points. *Proceedings of the National Academy of Sciences, 118*, Article e2106140118.
Choi, T.-M., Chan, H. K., & Yue, X. (2016). Recent development in big data analytics for business operations and risk management. *IEEE Transactions on Cybernetics, 47*, 81–92.
Commission, N.R., 1999. Technical basis and implementation guidelines for a technique for human event analysis (ATHEANA). NUREG-1624.
Ding, L., Zhou, C., Deng, Q., Luo, H., Ye, X., Ni, Y., & Guo, P. (2013). Real-time safety early warning system for cross passage construction in Yangtze Riverbed Metro Tunnel based on the internet of things. *Automation in Construction, 36*, 25–37.
Dolores, & Gracja, P. (2018). Human factor in flight safety. *Hadmérnök, 13*, 381–396.
Dzinyela, R., Alnawmasi, N., Adanu, E. K., Dadashova, B., Lord, D., & Mannering, F. (2024). A multi-year statistical analysis of driver injury severities in single-vehicle freeway crashes with and without airbags deployed. *Analytic Methods in Accident Research, 41*, Article 100317.
Endsley, M. R. (2021). Situation awareness. In *Handbook of human factors ergonomics* (pp. 434–455).
Flach, J. M. (1995). Situation awareness: Proceed with caution. *Human factors, 37*, 149–157.
French, S., Bedford, T., Pollard, S. J., & Soane, E. (2011). Human reliability analysis: A critique and review for managers. *Safety Science, 49*, 753–763.
Ghoul, T., Sayed, T., & Fu, C. (2023). Real-time safest route identification: Examining the trade-off between safest and fastest routes. *Analytic Methods in Accident Research, 39*, Article 100277.
Guo, Y., Sun, Y., He, Y., Du, F., Su, S., & Peng, C. (2022). A data-driven integrated safety risk warning model based on deep learning for civil aircraft. *Transactions on Aerospace Electronic Systems, 59*, 1707–1719.
Hamer, R., Waterson, P., & Jun, G. T. (2021). Human factors and nuclear safety since 1970–A critical review of the past, present and future. *Safety Science, 133*, Article 105021.
Hollnagel, E. (1998). *Cognitive reliability and error analysis method (CREAM)*. Elsevier.
Hollnagel, E. (2018). *Safety-I and safety-II: The past and future of safety management*. CRC Press.
Horita, F. E., de Albuquerque, J. P., & Marchezini, V. (2018). Understanding the decision-making process in disaster risk monitoring and early-warning: A case study within a control room in Brazil. *International Journal of Disaster Risk Reduction, 28*, 22–31.
IATA. (2021). *Safety report 2020*. Montreal, Canada: International Air Transport Association.
IATA. (2023). *Safety report 2022*. Montreal, Canada: International Air Transport Association.
ICAO. (2024). *Safety report*. Montreal Canada: International Civil Aviation Organization.
Jarvis, S., & Harris, D. (2010). Development of a bespoke human factors taxonomy for gliding accident analysis and its revelations about highly inexperienced UK glider pilots. *Ergonomics, 53*, 294–303.
Kelly, K. S., & Krzysztofowicz, R. (1994). Probability distributions for flood warning systems. *Water Resources Research, 30*, 1145–1152.
Krishna, K., & Murty, M. N. (1999). Genetic K-means algorithm. *Transactions on Systems, Man, Cybernetics, Part B, 29*, 433–439.
Li, S.-H., Cai, B.-G., Liu, J., & Wang, J. (2018). Collision risk analysis based train collision early warning strategy. *Accident Analysis & Prevention, 112*, 94–104.
Li, L., Gan, J., Yi, Z., Qu, X., & Ran, B. (2020). Risk perception and the warning strategy based on safety potential field theory. *Accident Analysis & Prevention, 148*, Article 105805.
Li, C., Sun, R., & Pan, X. (2023). Takeoff runway overrun risk assessment in aviation safety based on human pilot behavioral characteristics from real flight data. *Safety Science, 158*, Article 105992.
Li, H., Zhao, G., Qin, L., Aizeke, H., Zhao, X., & Yang, Y. (2020). A survey of safety warnings under connected vehicle environments. *IEEE Transactions on Intelligent Transportation Systems, 22*, 2572–2588.
Matsuo, K., Chigai, N., Chattha, M. I., & Sugiki, N. (2022). Vulnerable road user safety evaluation using probe vehicle data with collision warning information. *Accident Analysis & Prevention, 165*, Article 106528.
Mosleh, A., & Chang, Y. (2004). Model-based human reliability analysis: Prospects and requirements. *Reliability Engineering & System Safety, 83*, 241–253.
Oh, C., Oh, J.-S., & Ritchie, S. G. (2005). Real-time hazardous traffic condition warning system: Framework and evaluation. *IEEE Transactions on Intelligent Transportation Systems, 6*, 265–272.
Pan, X., Lin, Y., & He, C. (2017). A review of cognitive models in human reliability analysis. *Quality Reliability Engineering International, 33*, 1299–1316.
Poynter, A. (2023). *2022 CAR ACCIDENT DEATH STATISTICS*. USA: The National Highway Traffic Safety Administration.
Rasmussen, J. (1999). Ecological interface design for reliable human-machine systems. *The International Journal of Aviation Psychology, 9*, 203–223.
Reason, J. (1990). *Human error*. Cambridge University Press.
Saleh, J. H., Saltmarsh, E. A., Favarò, F. M., & Brevault, L. (2013). Accident precursors, near misses, and warning signs: Critical review and formal definitions within the framework of Discrete Event Systems. *Reliability Engineering & System Safety, 114*, 148–154.
Shappell, S., Detwiler, C., Holcomb, K., Hackworth, C., Boquet, A., & Wiegmann, D. A. (2017). Human error and commercial aviation accidents: An analysis using the human factors analysis and classification system. In *Human error in aviation* (pp. 73–88). Routledge.
Skybrary, 2024. Flight Crew Operating Manual (FCOM).
Summala, H. (1996). Accident risk and driver behaviour. *Safety Science, 22*, 103–117.
Sun, C., Wu, C., Chu, D., Zhong, M., Hu, Z., & Ma, J. (2016). Risk prediction for curve speed warning by considering human, vehicle, and road factors. *Transportation Research Record, 2581*, 18–26.
Sun, R., & Xiao, Y. (2012). Research on indicating structure for operation characteristic of civil aviation pilots based on QAR data. *Journal of Safety Science Technology, 8*, 49–54.
Swain, A. D. (1990). Human reliability analysis: Need, status, trends and limitations. *Reliability Engineering & System Safety, 29*, 301–313.
Tong, C., Yin, X., Li, J., Zhu, T., Lv, R., Sun, L., & Rodrigues, J. J. (2018). An innovative deep architecture for aircraft hard landing prediction based on time-series sensor data. *Applied Soft Computing, 73*, 344–349.
Wang, L., Wu, C., Sun, R., 2013. Pilot operating characteristics analysis of long landing based on flight QAR data. In *Engineering psychology and cognitive ergonomics. Applications and services: 10th international conference, EPCE 2013, held as part of HCI international 2013, Las Vegas, NV, USA, July 21-26, 2013, Proceedings, Part II 10* (pp. 157–166). Springer.
Wang, X., Wang, H., & Yu, L., 2018. Aircraft tail strike events during take-off phase: A risk evaluation model. In *2018 12th international conference on reliability, maintainability, and safety (ICRMS)* (pp. 142–145). IEEE.
Wang, L., Wu, C., & Sun, R. (2014). An analysis of flight Quick Access Recorder (QAR) data and its applications in preventing landing incidents. *Reliability Engineering & System Safety, 127*, 86–96.
Wen, H., Amin, M. T., Khan, F., Ahmed, S., Imtiaz, S., & Pistikopoulos, E. (2023). Assessment of situation awareness conflict risk between human and AI in process system operation. *Industrial Engineering Chemistry Research, 62*, 4028–4038.
Wickens, C. D., Helton, W. S., Hollands, J. G., & Banbury, S. (2021). *Engineering psychology and human performance*. Routledge.
Wu, J.-D., & Chen, T.-R. (2008). Development of a drowsiness warning system based on the fuzzy logic images analysis. *Expert Systems with Applications, 34*, 1556–1561.
Xiangzhang, W., He, W., & Bohao, X. (2024). Prediction of civil aircraft hard landing risk based on GBDT-GS method. *Journal of Applied Artificial Intelligence, 1*, 409–421.
Youlong, X., Wan, L., Lixin, Z., Feng, J., Hao, Z., Li, Z., & Yanhua, Z. (2023). Statistical analysis and suggestions on human-related operating events of nuclear power plants in recent five years. *Nuclear Safety, 22*, 49–54.
Yu, B., Bao, S., Chen, Y., & LeBlanc, D. J. (2021). Effects of an integrated collision warning system on risk compensation behavior: An examination under naturalistic driving conditions. *Accident Analysis & Prevention, 163*, Article 106450.
Zhang, R., Cai, L., Huang, D., & Gao, C. (2023). An advanced warning model of airplane hard landing based on Adaboost. *Journal of Physics: Conference Series*. IOP Publishing.
Zhang, Y., Chen, K., Weng, Y., Chen, Z., Zhang, J., & Hubbard, R. (2022). An intelligent early warning system of analyzing Twitter data using machine learning on COVID-19 surveillance in the US. *Expert Systems with Applications, 198*, Article 116882.
Zhirabok, A., Kalinina, N., & Shumskii, A. (2018). Technique of monitoring a human operator's behavior in man-machine systems. *Journal of Computer and Systems Sciences International, 57*, 443–452.